British Journal of Pharmacology

DOI:10.1111/j.1476-5381.2012.02211.x
www.brjpharmacol.org

RESEARCH PAPER

A novel compound, denosomin, ameliorates spinal cord injury via axonal growth associated with astrocyte-secreted vimentin

Kiyoshi Teshigawara[1]*, Tomoharu Kuboyama[1]*, Michiko Shigyo[1], Aiko Nagata[1], Kenji Sugimoto[2], Yuji Matsuya[2] and Chihiro Tohda[1]

[1]*Division of Neuromedical Science, Department of Bioscience, Institute of Natural Medicine, University of Toyama, Toyama, Japan, and* [2]*Laboratory of Synthetic Medical Chemistry, Faculty of Pharmaceutical Sciences, University of Toyama, Toyama, Japan*

Correspondence
Chihiro Tohda, Division of Neuromedical Science, Department of Bioscience, Institute of Natural Medicine, University of Toyama, 2630 Sugitani, Toyama 930-0194, Japan. E-mail: chihiro@inm.u-toyama.ac.jp

*These authors contributed equally to this work.

Keywords
spinal cord injury; axonal growth; Denosomin; reactive astrocyte; vimentin; 5-HT fibre

Received
19 June 2012
Revised
7 August 2012
Accepted
5 September 2012

BACKGROUND AND PURPOSE

In the spinal cord injury (SCI) axon regeneration is inhibited by the glial scar, which contains reactive astrocytes that secrete inhibitory chondroitin sulphate proteoglycan (CSPG). We previously reported that a novel compound, denosomin, promotes axonal growth under degenerative conditions in cultured cortical neurons. In this study, we investigated the effects of denosomin on functional recovery in SCI mice and elucidated the mechanism though which denosomin induces axonal growth in the injured spinal cord.

EXPERIMENTAL APPROACH

Denosomin was administered p.o. for 7 or 14 days to contusion mice. Behavioural evaluations and immunohistochemistry were done. Primary cultured cortical neurons and astrocytes were treated with denosomin to investigate the mechanism of axonal growth facilitation.

KEY RESULTS

Denosomin improved hind limb motor dysfunction and axonal growth, especially in the 5-HT-positive tracts across the scar and increased the density of astrocytes. Denosomin increased astrocyte proliferation, inhibited astrocytic death and increased the expression and secretion of vimentin in cultured astrocytes. Furthermore, vimentin increased axonal outgrowth in cultured neurons, even in the presence of inhibitory CSPG. Denosomin increased the number of vimentin-expressing astrocytes inside glial scars of SCI mice, and 5-HT-positive axonal growth occurred in a vimentin-associated manner.

CONCLUSION AND IMPLICATIONS

Denosomin increased the ratio of astrocytes that secrete vimentin as an axonal growth facilitator, which, we propose enhances axonal growth beyond the glial scar and promotes functional recovery in SCI mice. This study is the first to demonstrate this novel role of vimentin in SCI and drug-mediated modification of the inhibitory property of reactive astrocytes.

Abbreviations

ACM, astroglial conditioned medium; BMS, Basso Mouse Scale; BrdU, 5-bromo-2′-deoxyuridine; BSS, Body Support Scale; DAPI, 4′,6-diamidino-2-phenylindole; GFAP, glial fibrillary acidic protein; MAP2, microtubule-associated protein 2; NF-H, neurofilament-H; pNF-H, phosphorylated neurofilament-H; SCI, spinal cord injury

Introduction

Approximately 270 000 people in U.S. suffer from spinal cord injury (SCI) (Spinal Cord Injury Facts and Figures at a Glance, http://www.nscisc.uab.edu/), for which no effective drug therapy currently exists. SCI causes serious locomotor dysfunction due to the disruption of the descending motor and ascending sensory tracts at the lesion site. Several studies have suggested that the CNS has the ability to regenerate and that the regrowth of injured and/or spared axons may lead to recovery from locomotor dysfunction (David and Aguayo, 1981). However, the environment of the injured spinal cord inhibits axonal regeneration (Silver and Miller, 2004).

The formation of a glial scar, which is composed primarily of reactive astrocytes and with a marked expression of glial fibrillary acidic protein (GFAP) (Bignami and Dahl, 1974; Barrett *et al.*, 1981; Eng, 1985), at the lesion site in response to injury is believed to be a major impediment to axonal regeneration after SCI and other forms of CNS injury (Davies *et al.*, 1997; Silver and Miller, 2004; Yiu and He, 2006). At the lesion site, not only does the glial scar constitute a physical barrier to axonal growth, but the reactive astrocytes produce inhibitory extracellular matrix molecules such as chondroitin sulphate proteoglycan (CSPG) (McKeon *et al.*, 1991; Jones *et al.*, 2003). However, several lines of evidence suggest that reactive astrocytes in glial scars may possess important beneficial functions for stabilizing fragile CNS tissue after injury including the restriction of inflammation and the promotion of neuronal survival (Faulkner *et al.*, 2004; Okada *et al.*, 2006; Herrmann *et al.*, 2008; Rolls *et al.*, 2009). Reactive astrocytes, by producing various neurotrophic factors and cytokines, also exhibit adaptive plasticity (Aubert *et al.*, 1995; Ridet *et al.*, 1997) and are able to restore the extracellular ionic environment (Syková *et al.*, 1992).

We previously synthesized a novel compound, denosomin (Figure 1) that is an analogous derivative of sominone (Matsuya *et al.*, 2009) and is hydrophobic (CLogP = 4.9803). Sominone is a sapogenin metabolized from withanoside IV, which is one of the constituents of an ayurvedic tonic medicine Ashwagandha (root of *Withania somnifera* Dunal) (Kuboyama *et al.*, 2006), and is itself a constituent of Ashwagandha (Atta-ur-Rahman *et al.*, 1992). Our previous data showed that denosomin enhances axonal length in cultured cortical neurons, even after axonal dystrophy had been induced by amyloid β(1–42) treatment (Matsuya *et al.*, 2009). Therefore, we expected to find that denosomin induces axonal growth in the lesion site in SCI.

In the present study, we investigated the *in vivo* activities of denosomin in SCI mice and the underlying mechanism for its effects on axonal growth in the detrimental environment of injured spinal cord. Our results demonstrated that denosomin increases astrocyte density in the injured region of SCI mice and is able to convert one property of reactive astrocytes into a stimulant for axonal growth. We also clarified that denosomin-induced expression and secretion of the intermediate filament protein, vimentin, in astrocytes enhanced axonal growth and functional recovery in SCI mice. Altering the roles of astrocytes by medication may prove to be a very effective route for achieving SCI recovery and should be the focus of new therapeutic intervention strategies.

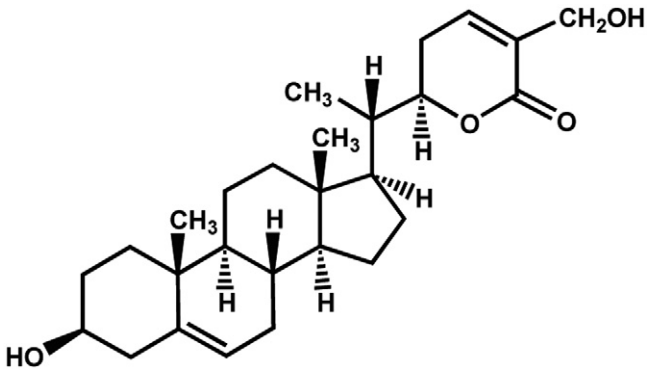

Figure 1
Structure of denosomin.

Methods

All studies involving animals are reported in accordance with the ARRIVE guidelines for reporting experiments involving animals (Kilkenny *et al.*, 2010; McGrath *et al.*, 2010). All experiments were performed in accordance with the Guidelines for the Care and Use of Laboratory Animals at the Sugitani Campus of the University of Toyama and the NIH Guidelines for the Care and Use of Laboratory Animals. The Committee for Animal Care and Use at the Sugitani Campus of the University of Toyama approved each of the study protocols. All efforts were made to minimize the number of animals used.

Animals and SCI model experiments

Seven-week-old male ddY mice (SLC) were used for the SCI experiments (total number of mice used = 50). The mice were housed with *ad libitum* access to food and water and were maintained under constant environmental conditions (22 ± 2°C, 50 ± 5% humidity and 12 h light : 12 h dark cycle starting at 07 h 00 min). The mice were anaesthetized by administration of trichloroacetaldehyde monohydrate (500 mg·kg^{-1}, i.p.). After the mice had completely lost their righting reflex, the surgical operations to produce SCI were performed, as described previously (Krenz and Weaver, 2000) with slight modifications. Contusion injuries were produced by twice dropping a 6.5 g weight from a height of 3 cm onto the exposed dura mater of the lumbar spinal cord L1 level using a stereotaxic instrument (Narishige, Tokyo, Japan). One hour after surgery, the SCI mice were randomly divided into the vehicle-treated and denosomin-treated groups, and application of the drug was initiated. Denosomin at 10 μmol·kg^{-1} (Figure 3A–D) or 20 μmol·kg^{-1} (Figures 2, 3E–H and 8–10) or a vehicle control was administered p.o. once daily to the animals for 7 days (Figures 8–10) or 14 days (Figures 2 and 3). For behavioural scoring, the mice were individually placed in an open field (23.5 cm × 16.5 cm × 12.5 cm) and observed for 5 min. Open-field locomotion was evaluated using the 0–9-point Basso Mouse Scale (BMS) locomotion scale and the 0–4-point Body Support Scale (BSS) locomotion scale.

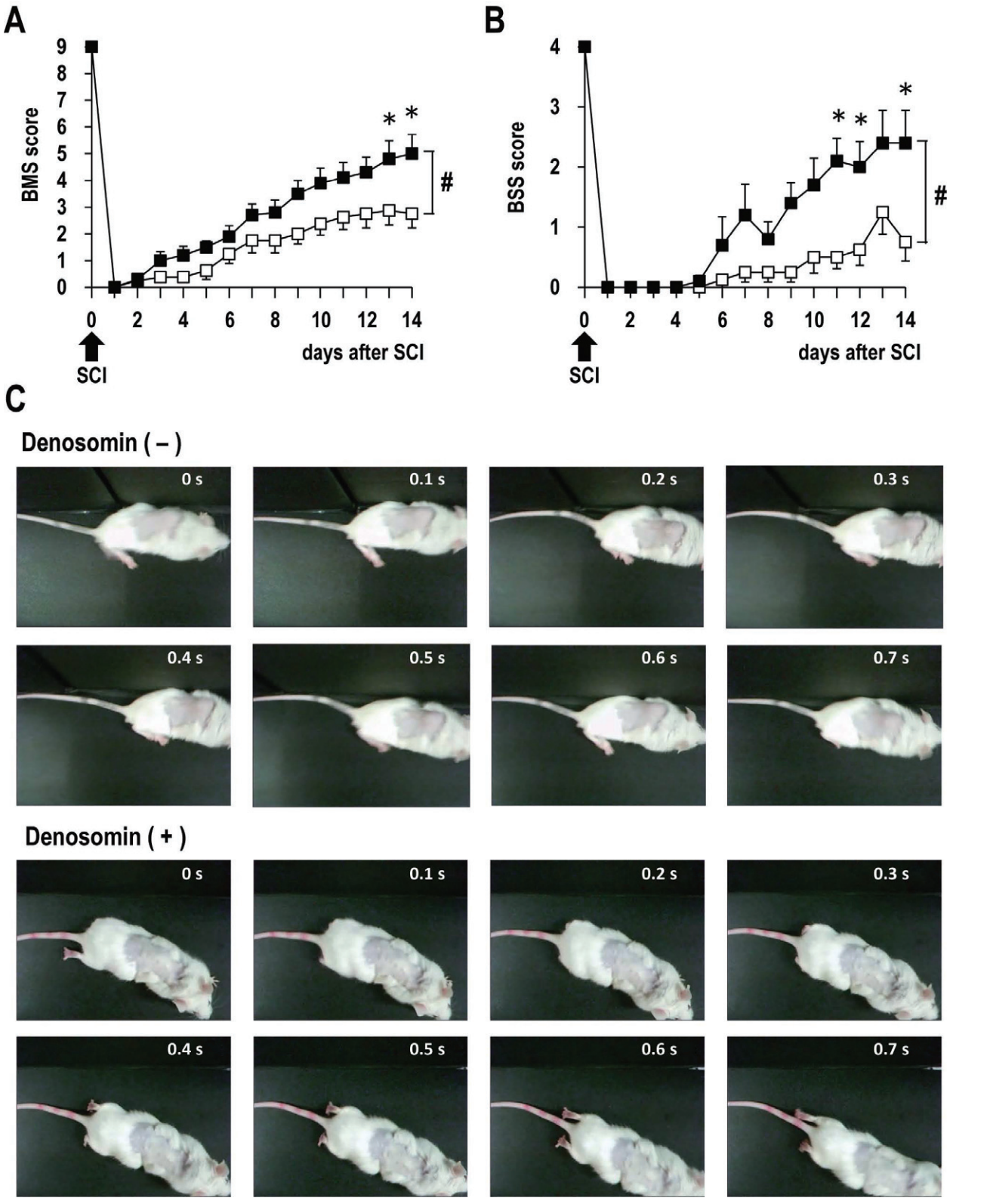

Figure 2

Denosomin enhances hind limb function in SCI mice. BMS (A) and BSS (B) scores were measured. SCI mice were administered denosomin (open squares, 4 mice, 8 hind limbs, $n = 8$) or vehicle solution (closed squares, 5 mice, 10 hind limbs, $n = 10$). At 14 days after the SCI, the movements of the mice were captured during walking. Sequentially captured images for 0.7 s are shown in (C). Also see movies 1 and 2. $^{\#}P = 0.0005$, drug × day interaction was analysed using a repeated measures two-way ANOVA, $F_{(14,\ 244)} = 2.89$; $^{*}P < 0.05$, compared to the vehicle-treated control SCI mice on the same day; *post hoc* Bonferroni test.

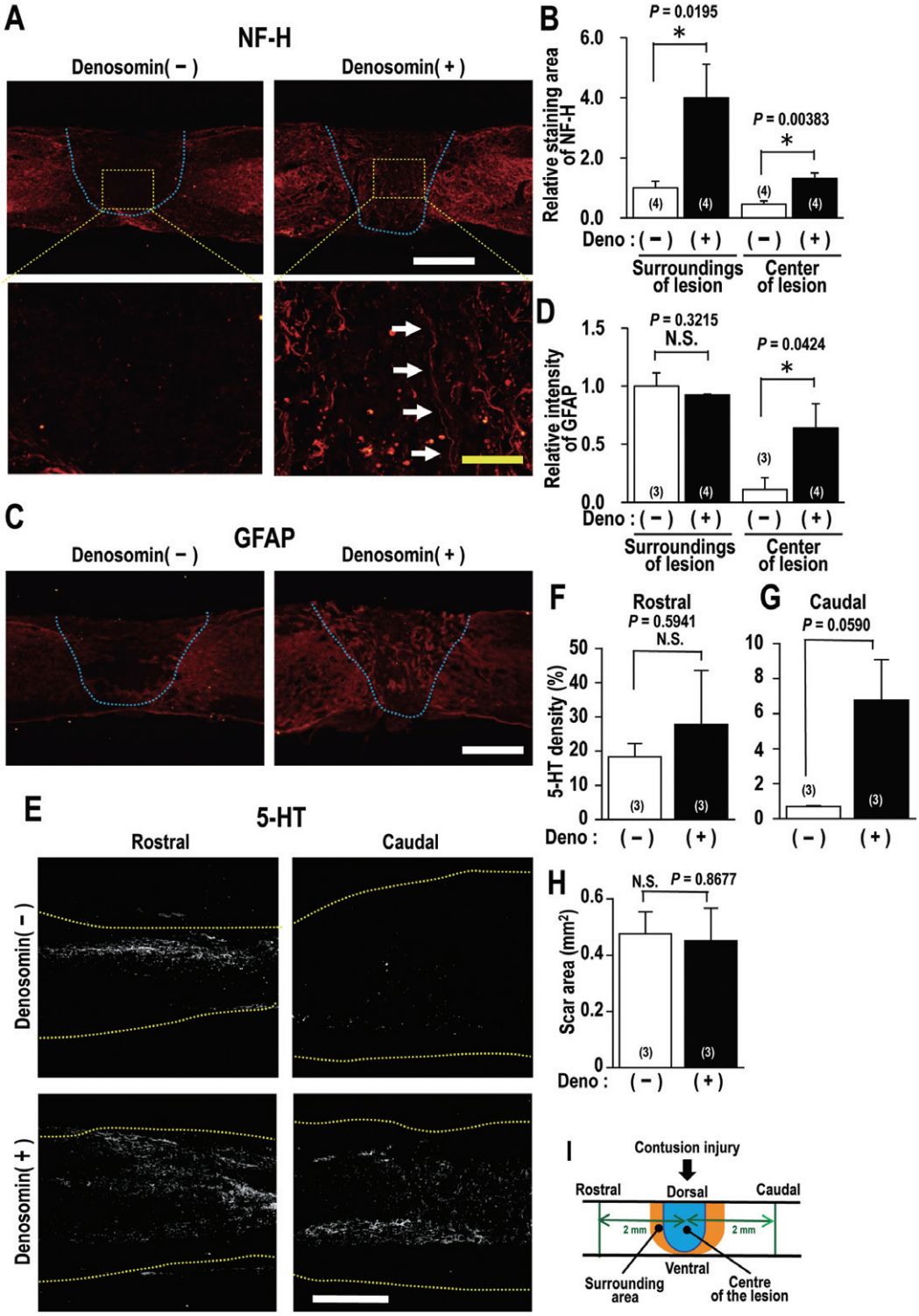

Figure 3

Denosomin enhances axonal density and reactive astrocytes in SCI mice. Sagittal sections of the spinal cord of vehicle- or denosomin-treated SCI mice were immunostained for NF-H (A), GFAP (C) or 5-HT (E). The relative areas of immunostaining for NF-H (B) or GFAP (D) were quantified in two locations of the spinal cord: at the centre of the lesion and in the adjacent sections (I). The lower panels in (A) are magnified images of the lesion centre. Arrows indicate the NF-H-positive axonal filaments. The blue dashed lines in (A) and (C) indicate the outlines of the glial scar. The dashed lines in (E) indicate the outlines of the spinal cords. The 5-HT-positive areas were measured at rostral and caudal sections 2 mm from the injury centre (I). The 5-HT-positive axonal densities in the rostral (F) and caudal (G) regions were quantified. (H) The sizes of glial scars were measured at the lesion centre in the slices used in (E–G). *$P < 0.05$, Student's unpaired *t*-test (two-tailed); N.S., not significant. The numbers of mice are shown in parentheses in the columns. The white scale bars indicate 500 μm, and the yellow bar indicates 200 μm.

Antibodies

The primary antibodies for immunohistochemistry included a rabbit anti-neurofilament-H (NF-H) polyclonal antibody (dilution 1:500; Chemicon, Temecula, CA, USA), a mouse anti-GFAP monoclonal antibody (clone 1D4, dilution 1:1000; Applied Biological Materials, Richmond, BC, Canada), a rabbit anti-5-HT polyclonal antibody (dilution 1:1000; ImmunoStar, Hudson, WI, USA), a mouse anti-vimentin monoclonal antibody (clone RV202, dilution 1:100; Santa Cruz Biotechnology, Santa Cruz, CA, USA), a mouse anti-CSPG monoclonal antibody (clone CS-56, dilution 1:500; Sigma, St. Louis, MO, USA), a rabbit anti-laminin polyclonal antibody (dilution 1:1000; Biomedical Technologies, Stoughton, MA, USA), a rabbit anti-β-actin polyclonal antibody (dilution 1:1000; Cell Signaling Technology, Danvers, MA, USA), a mouse anti-phosphorylated NF-H (pNF-H) monoclonal antibody (clone: SMI-35, dilution 1:500; Covance, Emeryville, CA, USA), a rabbit anti-microtubule associated protein 2 (MAP2) polyclonal antibody (dilution 1:500; Chemicon), a rabbit anti-GFAP polyclonal antibody (dilution 1:1000; Dako, Glostrup, Denmark) and a 5-bromo-2′-deoxyuridine (BrdU) monoclonal antibody (clone: Mobu-1, dilution 1:500; Merck Calbiochem, Darmstadt, Germany). The secondary antibodies used were Alexa Fluor 488- or 594-conjugated goat anti-mouse IgG (dilution 1:300), Alexa Fluor 350-conjugated goat anti-mouse IgM (dilution 1:300), Alexa Fluor 594-conjugated goat anti-mouse IgG1 (dilution 1:300) and Alexa Fluor 488- or 568-conjugated goat anti-rabbit IgG (dilution 1:300; Invitrogen, Carlsbad, CA, USA).

Immunohistochemistry

After behavioural scoring, serial spinal cord slices were obtained as 10 μm sagittal sections to determine the expression therein of NF-H, GFAP, vimentin, 5-HT, CSPG, laminin and β-actin; and these samples were also counterstained with DAPI (Biomol, Farmingdale, NY, USA). The fluorescent images shown in Figure 3A, C and E were captured at 320 μm × 420 μm or 1600 μm × 2100 μm using a fluorescence microscope (BX-61/DP70, Olympus, Tokyo, Japan). The densities of NF-H-positive axons and GFAP-positive astrocytes were measured using an ATTO densitography image analyser (ATTO, Tokyo, Japan). Ten randomly selected 100 μm × 100 μm squares in the centres of the lesions or adjacent to the lesions were measured to calculate the average value per slice (Figure 3B and D). The fluorescent images in Figure 3E–G were captured at distances of 2 mm rostral and caudal from the injury centre (Figure 3I) at 1600 μm × 2100 μm using a BX-61/DP70 microscope. The fluorescent images in Figures 8–10 were captured at 106 μm × 142 μm (Figure 8) or at 670 μm × 890 μm (Figures 9 and 10) using a fluorescence microscopy system (Axio observer Z1, Carl Zeiss, Oberkochen, Germany). The densities of the 5-HT-, vimentin-, GFAP- and CSPG-positive areas inside of the scar were determined using the ImageJ image analyser (NIH). An observer, blind to the different treatments, determined the threshold values and ROIs (Figures 3F,G, 9 and 10). The GFAP-positive regions (Figure 3) and CSPG-positive regions (Figures 9 and 10) of the scar were then quantified.

Primary culture

Primary cultured spinal cord and cerebral cortical cells were prepared from the E17-18 embryos of 30 Sprague–Dawley rats (SLC, Hamamatsu, Shizuoka, Japan) at a density of 1.45–1.74 × 10^5 cells·cm^{-2} or E14 embryos of three ddY mice (SLC) at a density of 1.45–4.35 × 10^4 cells·cm^{-2} (Figure 7I–K) as described previously (Kuboyama *et al.*, 2005) with modifications. Neurons and astrocytes coexisted in our culture conditions (data not shown). The cells were cultured in eight-well chamber slides (Falcon, Franklin Lakes, NJ, USA). Cortical and spinal cell cultures were given Neurobasal medium (Invitrogen) containing 2% B-27 supplement (Invitrogen), 0.6% D-glucose and 2 mM L-glutamine. Axonal densities were analysed by immunocytochemistry for pNF-H and MAP2 following Denosomin (Matsuya *et al.*, 2009) or vimentin (ProSpec, Rehovot, Israel) treatment.

Rat spinal cord astrocytes were cultured as described previously (McCarthy and de Vellis, 1980) with modifications. Rat spinal cord cells (E17-18) were cultured for 12–14 days with shaking in T-25 flasks (Falcon) in DMEM/F12 (1:1) medium (Invitrogen) containing 10% FBS. Microglia and oligodendrocyte precursor cells were detached by shaking. Immunocytochemistry indicated that the percentage of GFAP-positive astrocytes was greater than 95% using our procedure, and the remaining cells were microglia. Purified astrocytes were seeded in eight-well chamber slides coated with 5 μg·mL^{-1} poly-D-lysine (PDL) at a density of 0.72–1.45 × 10^5 cells·cm^{-2}. T-25 flasks were coated with 5 μg·mL^{-1} PDL. The eight-well chamber slides were coated with 5 μg·mL^{-1} PDL following treatment with 0.5 μg·mL^{-1} aggrecan (Sigma), which is a CSPG (Figure 7J and K). Fluorescent images were captured at 670 μm × 890 μm using the BX61/DP70 microscope. Axons were automatically detected by the Neurocyte image analyser (Kurabo, Osaka, Japan), and the densities of axons per neuron were calculated. An observer, blind to the different treatments, captured and analysed the images (Figure 7I and K).

BrdU incorporation assay

Cellular proliferation was evaluated using the BrdU incorporation assay. BrdU (Sigma) was added to the culture medium for 24 h at a final concentration of 10 μM. The cells were incubated in 2 M HCl for 20 min at 37°C after fixation and were washed in 0.1 M borate buffer. The cells were immunostained for BrdU and counterstained with DAPI.

TUNEL assay

H_2O_2 (at a final concentration of 300 μM) was added to the astrocyte culture medium for 24 h. The proportion of cells that exhibited cellular death was determined using the *In Situ* Cell Death Detection Kit (Roche, Mannheim, Germany) according to the manufacturer's protocol.

Cell migration assay

Isolated astrocytes were cultured until fully confluent (a state of growth arrest) for 7 days to avoid the influence of cell proliferation activity. The central part of the astroglial layer was then scratched using a 1.5 mL Pipette tip. The scratched cell-free area was observed for 3 days after the scratch wound and was recorded with a phase-contrast microscope. Subsequently, astrocytes were immunostained for GFAP and counterstained with DAPI.

ELISA for vimentin

Cultured rat astrocytes were treated with vehicle solution or 1 μM denosomin for 5 days in DMEM/F12 (1:1) containing

10% FBS, and the astrocytes were treated for 1 day with denosomin-free and serum-free neurobasal medium. Conditioned medium (ACM) and astrocyte lysates were collected individually. The cells were lysed using a lysis buffer (pH 7.5, 140 mM NaCl, 50 mM Tris–HCl, 1% NP-40, 10 mM EDTA, 20 mM NaF, 20 mM β-glycerophosphate, 1 mM PMSF, 1 mM DTT, 1 mM sodium vanadate and a protease inhibitor cocktail; Roche). The vimentin concentrations in these samples were quantified using a rat vimentin ELISA kit according to the manufacturer's protocol (Cusabio Biotech, Wuhan, Hubei, China).

Statistical analysis

Statistical comparisons were performed using a one-way ANOVA followed by the *post hoc* Dunnett's test, or using a repeated measures two-way ANOVA followed by the *post hoc* Bonferroni test and an unpaired (two-tailed) *t*-test. The Prism 5 (GraphPad software) programme was used for the statistical analyses. *P*-values <0.05 were considered significant. The mean values of the data are presented along with the SEM.

Results

Administration of denosomin, p.o., induced increases in astrocytes, axonal growth and functional recovery in SCI mice

Mice with contusion SCI were administered denosomin, p.o., for 14 consecutive days following injury. Motor function of two hind limbs was separately scored using the BMS, which evaluates ankle movement and walking stability (Basso *et al.*, 2006) (Figure 2A), along with criteria we developed to assess the degree of hind limb muscle strength for support of the body trunk, that is the BSS (see Table 1 and Figure 2B). Most SCI mice displayed complete bilateral hind limb paralysis the day after injury. Denosomin-treated SCI mice displayed improvements in hind limb function during the first week. At 14 days after the SCI, denosomin-treated mice showed high mobility of their hind limb ankles during walking, but vehicle-treated mice had little movement in their ankles (Figure 2C; Supporting Information Movies S1,S2). The BMS and BSS scores of denosomin-treated mice gradually and significantly increased compared with control SCI mice over the 14 day course of administration (Figure 2A and B). We repeated these experiments were repeated more than three times and confirmed that a similar degree of motor dysfunction was reproducibly observed in our contusion model. The pattern of spontaneous recovery of the motor function, which reached a plateau (2–3 in BMS score) at 14 days after the injury, and the effectiveness of denosomin were also reproducible (data not shown). Denosomin administration did not affect the body weight or induce abnormal behaviours in mice (data not shown).

Table 1

Operational definitions of the BSS scale

Score	Criteria
0	No ankle movement or slight ankle movement, and no touching of the sole on the floor
1	Extensive ankle movement, touching of the sole on the floor, but no support of the body trunk
2	Touching of the sole on the floor, no support of the body trunk, sometimes support of hindquarters
3	Touching of the sole on the floor, always support of the body trunk, unstable weight support
4	Touching of the sole on the floor, always support of the body trunk, stable weight support

The injured spinal cords of denosomin-treated (for 14 days) SCI mice were then histologically examined. In vehicle-treated SCI mice, NF-H (an axonal marker)-positive staining showed that axons were lost around the centre of the lesion and its surroundings (Figure 3A). The areas of NF-H-positive axons were measured in the centre of the lesion and the adjacent locations (Figure 3I). Axonal density was significantly increased in both the lesion centres and the adjacent sections in the spinal cords of denosomin-treated SCI mice (Figure 3B). Next, spinal cord slices were immunostained for 5-HT (Figure 3E–G), which is a marker of the 5-hydroxytryptaminergic raphespinal tract in the spinal cord, because the raphespinal tract largely regulates locomotive function (Jacobs *et al.*, 2002). The 5-HT-positive areas were measured in the caudal and rostral regions at a distance of 2 mm from the injury centre (Figure 3I). The caudal 5-HT-positive axonal densities of animals in the denosomin group were greater than those of the vehicle group (Figure 3G), but the densities on the rostral sides did not differ notably (Figure 3F). At 7 days after denosomin administration, 5-HT-positive axons were increased in the lesion region but were rarely observed at the caudal site of the injury region (Figure 9A). These results suggest denosomin induces the axons in the glial scar (at least those in the raphespinal tracts) to elongate and towards the caudal site. Immunostaining for GFAP was performed to identify reactive astrocytes (Figure 3C and D). GFAP-positive astrocytes in SCI control mice were localized to the areas adjacent to the lesions. In contrast, GFAP-positive astrocytes in denosomin-treated SCI mice were located at the centre of the lesions as well as in areas adjacent to the lesions (Figure 3C). The sizes of the glial scars were not different between the control and denosomin-treated SCI mice (Figure 3H). The marked increment in GFAP-positive astrocytes in the lesion centre was significantly enhanced by denosomin administration (Figure 3D).

Denosomin increased astrocyte proliferation and reduced oxidative stress-induced astrocyte death but did not increase astrocyte migration

To assess the effect of denosomin treatment on astrocytes within the scar of SCI mice, astrocyte proliferation was investigated in pure cultures of astrocytes isolated from rat spinal cords. The astrocytes were cultured with denosomin. Six days later, BrdU incorporation, for 24 h, was assessed to evaluate any increases in astroglial proliferation. The number of BrdU-positive astrocytes was significantly increased after denosomin treatment (Figure 4A and B), and the total number of astrocytes also increased (Figure 4C). Furthermore, the growth rate of astrocytes and the ratio of BrdU-positive astro-

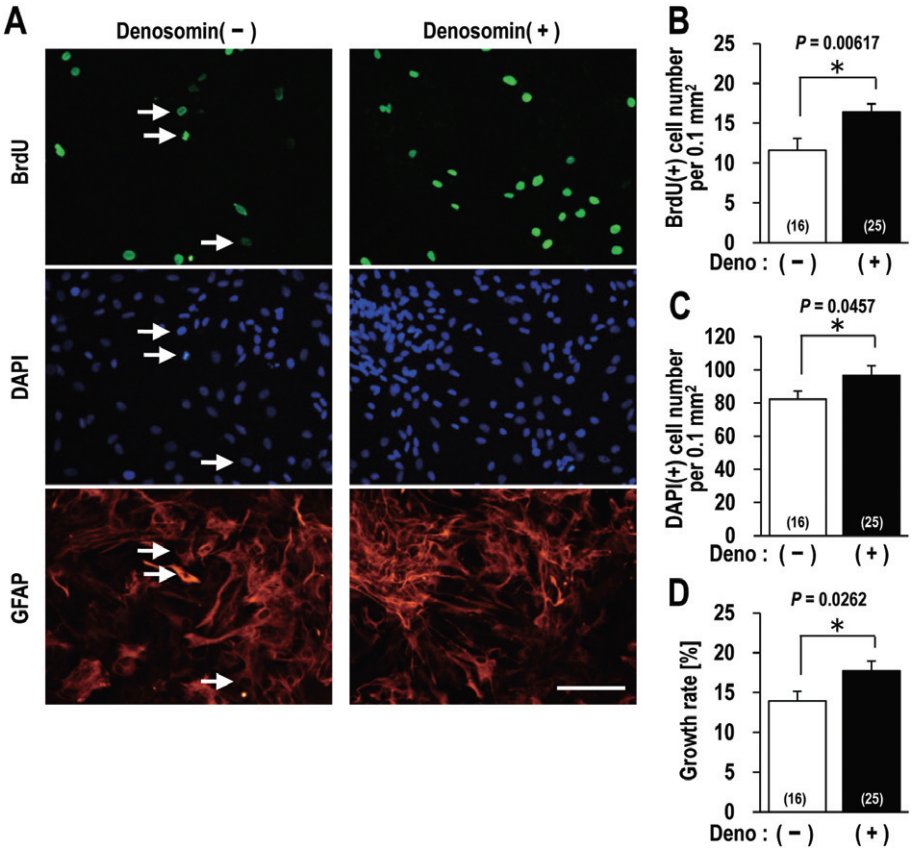

Figure 4

Denosomin enhances the proliferation of cultured astrocytes. Isolated astrocytes were cultured in the presence or absence of 1 μM denosomin (Deno) for 6 days and then treated with BrdU for 24 h. The astrocytes were immunostained for GFAP and BrdU and counterstained with DAPI (A). Astrocyte proliferation (B), total astrocyte number (C) and the astrocyte growth rate (D) were evaluated. Arrows indicate proliferating astrocytes (A). *$P < 0.05$, Student's unpaired *t*-test (two-tailed); #$P < 0.05$, compared to control cells without denosomin and H_2O_2, one-way ANOVA followed by *post hoc* Bonferroni test. The numbers of photos are shown in parentheses in the columns. The scale bar indicates 100 μm.

cytes to DAPI-positive astrocytes both significantly increased in response to denosomin (Figure 4D).

The primary mechanical damage associated with SCI is followed by a secondary injury phase that involves oxidative stress, inflammation and cell death (Rowland *et al.*, 2008; Olby, 2010). Thus, the effect of denosomin on astrocyte survival was investigated. Astrocyte death was induced *in vitro* by addition of H_2O_2 and it was then assessed using the TUNEL assay (Figure 5). Denosomin treatment was started 24 h before the addition of H_2O_2, and the TUNEL assays were performed at 24 h after the addition of H_2O_2. In untreated control astrocytes, almost no TUNEL-positive dead astrocytes were observed with or without denosomin treatment. In contrast, H_2O_2 treatment resulted in a significant increase in the number of TUNEL-positive astrocytes. Moreover, denosomin pretreatment of H_2O_2-treated astrocytes markedly and significantly decreased the number of TUNEL-positive astrocytes (Figure 5A and B). Denosomin significantly decreased the death rate of H_2O_2-treated astrocytes and the ratio of TUNEL-positive astrocytes to DAPI-positive astrocytes (Figure 5C). The promotion of astrocyte migration from outside of the scar is another possible explanation for the increase in astrocytes within the scar. Thus, an *in vitro* migration assay was performed (Figure 6). The number of astrocytes migrating into the scratched space (scar) did not differ in the presence or absence of denosomin.

Denosomin enhanced the secretion of vimentin from astrocytes, leading to axonal elongation

Reactive astrocytes in the glial scar are a major impediment to axonal regrowth (Davies *et al.*, 1997; Silver and Miller, 2004; Tom *et al.*, 2004; Yiu and He, 2006). However, axonal growth and reactive astrogliosis were enhanced in the lesion centres of denosomin-treated SCI mice (Figure 3), and similar phenomena were observed in denosomin-treated cultured cells (Figures 4, 5, Supporting Information Figures S1 and S2). Therefore, we hypothesized that the denosomin-induced increase in astrocytes does not inhibit axonal growth but rather assists in axonal crossing of the lesion scar. To investigate this hypothesis, spinal cord cells were cultured in denosomin-free medium and were also co-cultured with isolated denosomin-treated astrocytes (Figure 7C). The axonal densities of spinal cord neurons layered on denosomin-treated astrocytes were significantly increased when they

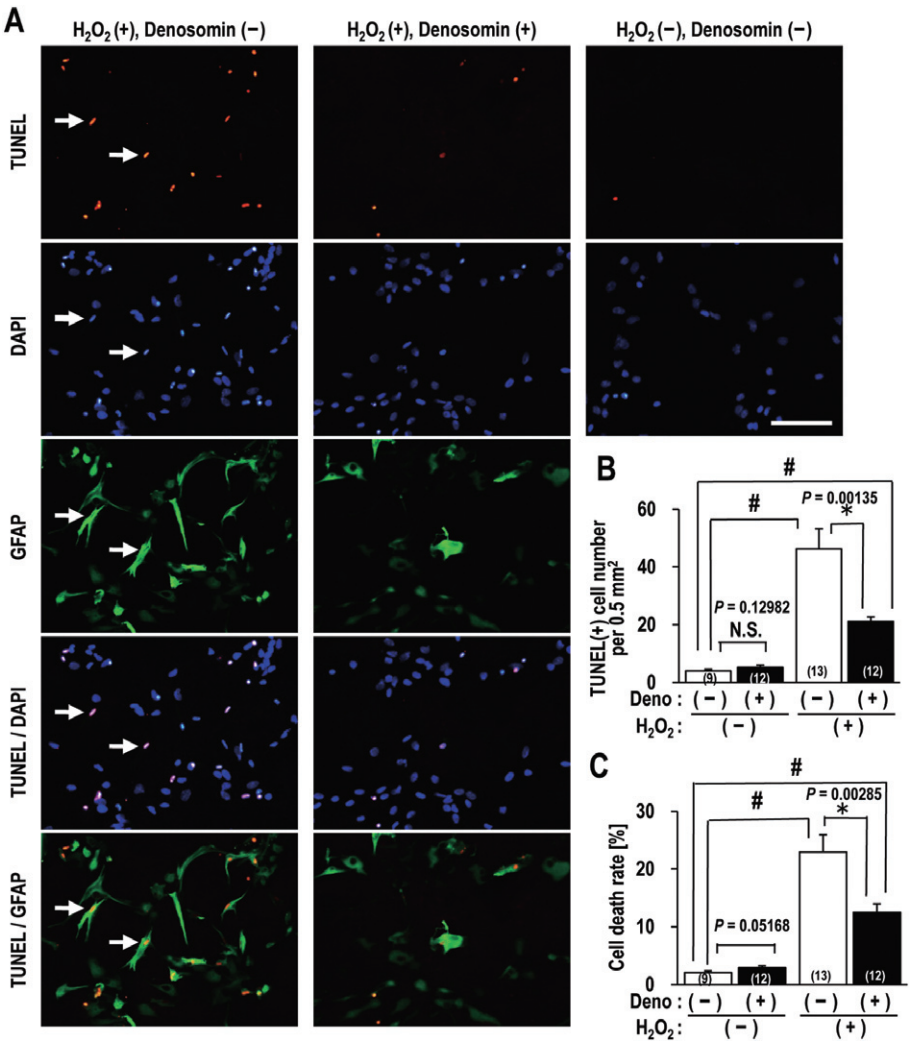

Figure 5

Denosomin inhibits the H_2O_2-induced death of cultured astrocytes. The isolated astroglial layer was pretreated with 1 μM denosomin (Deno) after 5 days of culture. Isolated astrocytes were treated with H_2O_2 for 24 h, and the TUNEL assay and GFAP immunostaining were then performed. All cells were counterstained with DAPI (A). Astrocyte death was evaluated by the quantification of TUNEL-positive cells (B). The rate of astrocyte death was evaluated using the ratio of TUNEL-positive astrocytes to DAPI-positive astrocytes (C). Arrows indicate dying astrocytes (A). $^{*}P < 0.05$, Student's unpaired *t*-test (two-tailed); $^{\#}P < 0.05$, compared to control cells without denosomin and H_2O_2, one-way ANOVA followed by *post hoc* Bonferroni test. The numbers of photos are shown in parentheses in the columns. The scale bar indicates 100 μm.

were not given direct denosomin stimulation (Figure 7A and B). Next, we investigated the dependence of astrocyte-mediated axonal outgrowth on astrocyte secretion. Cultured spinal cord cells were treated with astrocyte-conditioned medium (ACM) from astrocyte cultures that had been treated with denosomin for 6 days (Figure 7F). The axonal densities of the cultured spinal cord cells that were treated with denosomin-untreated, ACM for 6 days increased compared with those treated with control (non-ACM) medium (Figure 7D). Furthermore, denosomin-pretreated ACM significantly increased the axonal densities compared with the denosomin-untreated ACM group. The neuron number and non-neuronal cell number were not changed by the denosomin-pretreated ACM, (Figure 7E). These results demonstrate that denosomin-treated astrocytes secrete some factors that stimulate axonal elongation.

To identify the proteins that stimulated axonal elongation, the levels of astrocyte protein expression were exhaustively compared between the denosomin- and vehicle-treated astrocytes using two-dimensional (2D) PAGE (Supporting Information Figure S3) and LC-MS/MS analyses. These analyses revealed that levels of the intermediate filament protein vimentin notably increased in denosomin-treated astrocytes, and vimentin was found to produce the most dense band on the 2D-PAGE. An ELISA analysis further confirmed the increased vimentin levels in denosomin-treated astrocytes (Figure 7G). There were also increased vimentin levels in the ACM of denosomin-treated astrocytes (Figure 7H). The vimentin content in control astrocytes was 3.99 $ng \cdot mL^{-1}$ compared with 17.4 $ng \cdot mL^{-1}$ in denosomin-treated astrocytes. Calibration by protein concentrations showed vimentin concentrations were 0.55 $ng \cdot \mu g^{-1}$ protein and 1.93 $ng \cdot \mu g^{-1}$

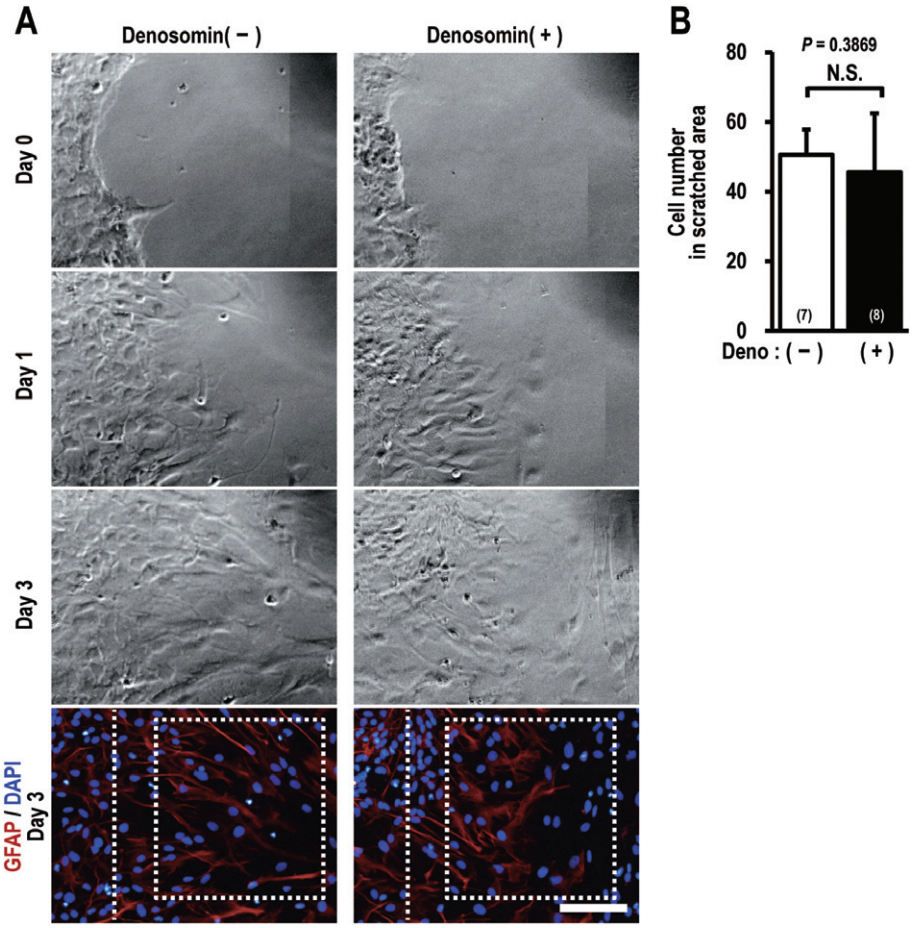

Figure 6

Denosomin does not influence cell migration in the scratched astroglial culture. After 6 days of culture, the isolated astroglial layer was pretreated with 1 μM denosomin (Deno). Twenty-four hours later, the layer was scratched. Astroglial migration into the scratched cell-free area was then observed for 3 days (A). Astrocytes were immunostained for GFAP and counterstained with DAPI 3 days after the scratch wounding. The number of migrated astrocytes in the cell-free area (surrounded by a dotted square) was quantified (B). A solid line delineates the edge of the astrocyte layer immediately adjacent to the scratch wound. N.S., Not significant in, unpaired *t*-test (two-tailed). The numbers of photos are shown in parentheses in the columns. The scale bar indicates 100 μm.

protein in cortical ACM and denosomin-treated ACM respectively. This indicates that the ratio of vimentin to total proteins in ACM was increased by denosomin, suggesting that it induces the secretion of vimentin.

In vivo, the distribution of vimentin primarily overlapped that of laminin, an extracellular matrix protein, inside the glial scars of denosomin-treated SCI mice (Figure 8A). The vimentin-positive areas also appeared to be outside β-actin (Figure 8B), which is a cytoplasmic protein that is also distributed at the plasma membrane (Hoock *et al.*, 1991). These distribution patterns strongly suggest that vimentin was being secreted in the spinal cord *in vivo*. Vimentin secretion from astrocytes (Greco *et al.*, 2010; Cordero-Llana *et al.*, 2011) and macrophages (Mor-Vaknin *et al.*, 2003; Xu *et al.*, 2004) has been reported previously. It has been proposed that vimentin interacts with the endoplasmic reticulum (ER) membrane and is selectively exported from the ER to the Golgi complex and then secreted (Mor-Vaknin *et al.*, 2003; Huet *et al.*, 2006). However, the functional significance of vimentin secretion with respect to neuronal activity is not known. The direct application of vimentin resulted in increase in axonal densities at 10 ng·mL^{-1} in primary cultured cortical neurons (Figure 7I), which was consistent with the concentration of vimentin in the ACM treated with denosomin (Figure 7H). Vimentin (10 ng·mL^{-1}) also significantly increased axonal densities even on inhibitory CSPG-coated slides (Figure 7J and K). These results are very important, because CSPG is deposited inside the glial scar and generally inhibits axonal regeneration in SCIs (Silver and Miller, 2004). Together, these results indicate that denosomin treatment increases vimentin expression and secretion by astrocytes, which then leads to the promotion of axonal growth.

Denosomin increased the vimentin-positive astrocyte frequency and axonal growth along vimentin-positive astrocytes in the injured regions of SCI mice

The expression and distribution of vimentin were further investigated *in vivo*. Spinal cord slices from SCI mice that had

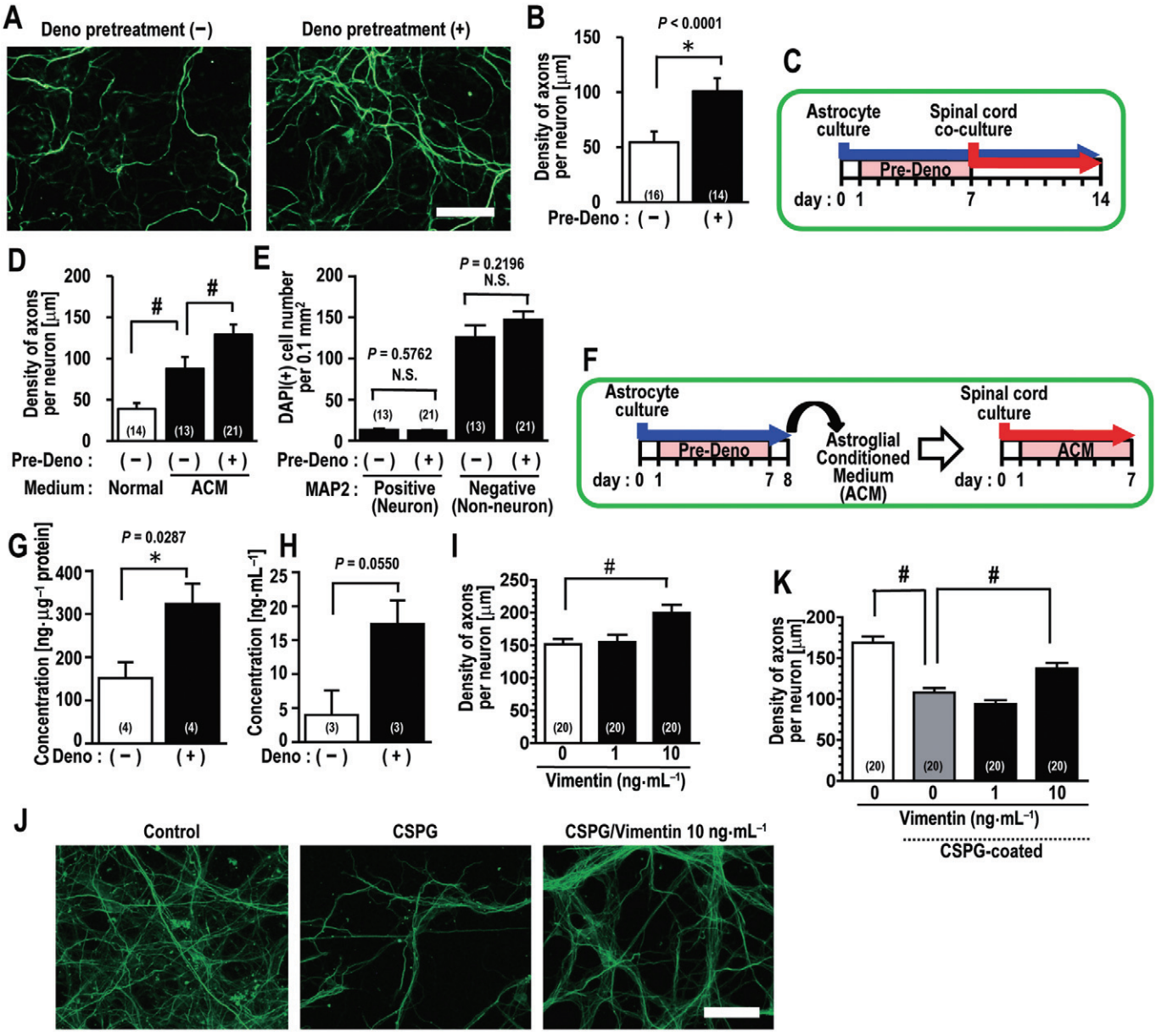

Figure 7

Denosomin-mediated axonal outgrowth in primary cultures is mediated by vimentin secretion from astrocytes. (A–C) Isolated astrocytes were cultured in the presence or absence of 1 μM denosomin (Pre-Deno) for 6 days. Rat spinal cord cells were cocultured on the astrocyte layer without denosomin for 7 days after the astrocytes had been treated with denosomin. (D–F) Isolated astrocytes were cultured in the presence or absence of 1 μM denosomin (Pre-Deno) for 6 days. The culture medium was then replaced with fresh medium without denosomin, and the medium was collected 24 h later for use as astrocyte-conditioned medium (ACM). Rat primary cultured spinal cord cells were cultured in normal medium or ACM for 6 days (F). (G and H) Cultured astrocytes that were treated with or without denosomin (Deno) (G) and ACM collected from the astrocyte culture (H) were used for the ELISA assay. (I–K) Isolated mouse cortical cells were cultured with or without 1 or 10 ng·mL^{-1} vimentin for 6 days. The cells were cultured on slides with (J and K) or without (I–J) a CSPG coating. The cells were immunostained for pNF-H and MAP2, and the densities of pNF-H-positive axons on each neuron were quantified (B, D, I and K). Cellular distributions of neurons and non-neuronal cells per 0.1 mm^2 were evaluated by the quantification of MAP2- and DAPI-positive cells (E). In (B, G and H): *P < 0.05, Student's unpaired t-test (two-tailed); $^{\#}P$ < 0.05; one-way ANOVA followed by the *post hoc* Bonferroni test, versus the control ACM treatment (D), versus the control cells (I) or versus CSPG-coated control cells (K). The numbers of photos (B, D, E, I, and K) or measurements (G and H) are shown in parentheses in the columns. The scale bar indicates 100 μm.

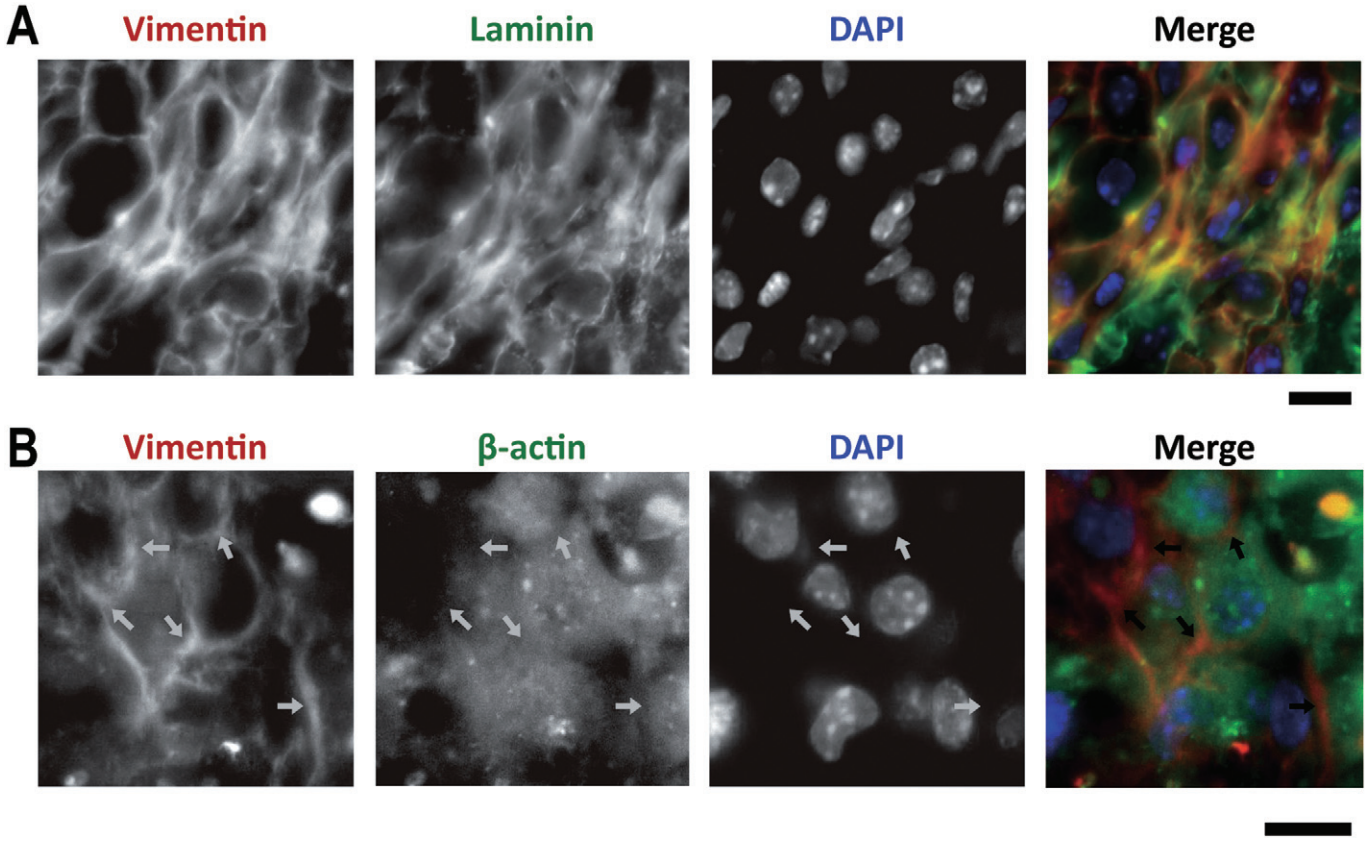

Figure 8

Vimentin is located primarily in the extracellular matrix inside the glial scar of SCI mice. Spinal cord slices of SCI mice that had been treated with denosomin were immunostained with antibodies for vimentin and laminin (extracellular matrix) (A) or vimentin and β-actin (cytoplasm and plasma membrane) (B). Both combinations were counterstained with DAPI. Arrows indicate gap space between cells. The scale bar indicates 10 μm.

been treated with denosomin for 7 days were immunostained for 5-HT and vimentin (Figure 9). The sizes of CSPG-positive glial scar areas were not significantly different between SCI control and denosomin-treated SCI mice (Figure 9C). The level of CSPG expressed was also not changed by denosomin (Figure 9D). Denosomin administration significantly increased the frequency of 5-HT-positive (Figure 9E) and vimentin-positive areas (Figure 9F) within the scar. Additionally, 5-HT axons were elongated along the scar rim where vimentin was highly expressed (Figure 9A). In control mice, 5-HT-positive axons rarely overlapped with vimentin-positive regions. In contrast, the majority of 5-HT-positive axons were co-localized with vimentin in denosomin-treated mice (Figure 9B). The frequency of 5-HT axons associating with vimentin significantly increased in the denosomin-treated group (Figure 9G). These results indicate that denosomin enhanced the raphespinal tract growth inside the scar, and this growth was probably due to an association of the raphespinal tracts with secreted vimentin or vimentin-positive cells.

The promotion and inhibition of axonal growth by reactive astrocytes has previously been well characterized (Silver and Miller, 2004; Okada *et al.*, 2006; Yiu and He, 2006; Rolls *et al.*, 2009; White *et al.*, 2011). To clarify that the conversion of astrocyte function relates to vimentin expression, spinal cord slices were immunostained for vimentin, CSPG and GFAP (Figure 10). Regions expressing vimentin mainly overlapped with GFAP-positive astrocytes along the scar rim (Figure 10A). Denosomin treatment significantly increased the frequency of astrocytes that were positive for GFAP and vimentin (Figure 10B and C), whereas this treatment did not significantly increase the frequency of astrocytes that were positive for CSPG and GFAP (Figure 10B and D). As shown in Figure 3C and D, denosomin increased the density of astrocytes in the scar. These findings suggest that denosomin specifically increases vimentin-positive astrocytes to promote axonal growth. However, denosomin did not affect the frequency of CSPG-positive astrocytes, which inhibit axonal growth.

Discussion and conclusions

We previously demonstrated that a novel compound, denosomin, has the potential to promote axonal growth and attenuate neuronal loss under the amyloid β(1–42)-induced neurodegenerative condition in primary cultured cortical neurons coexisting with astrocytes (Matsuya *et al.*, 2009).

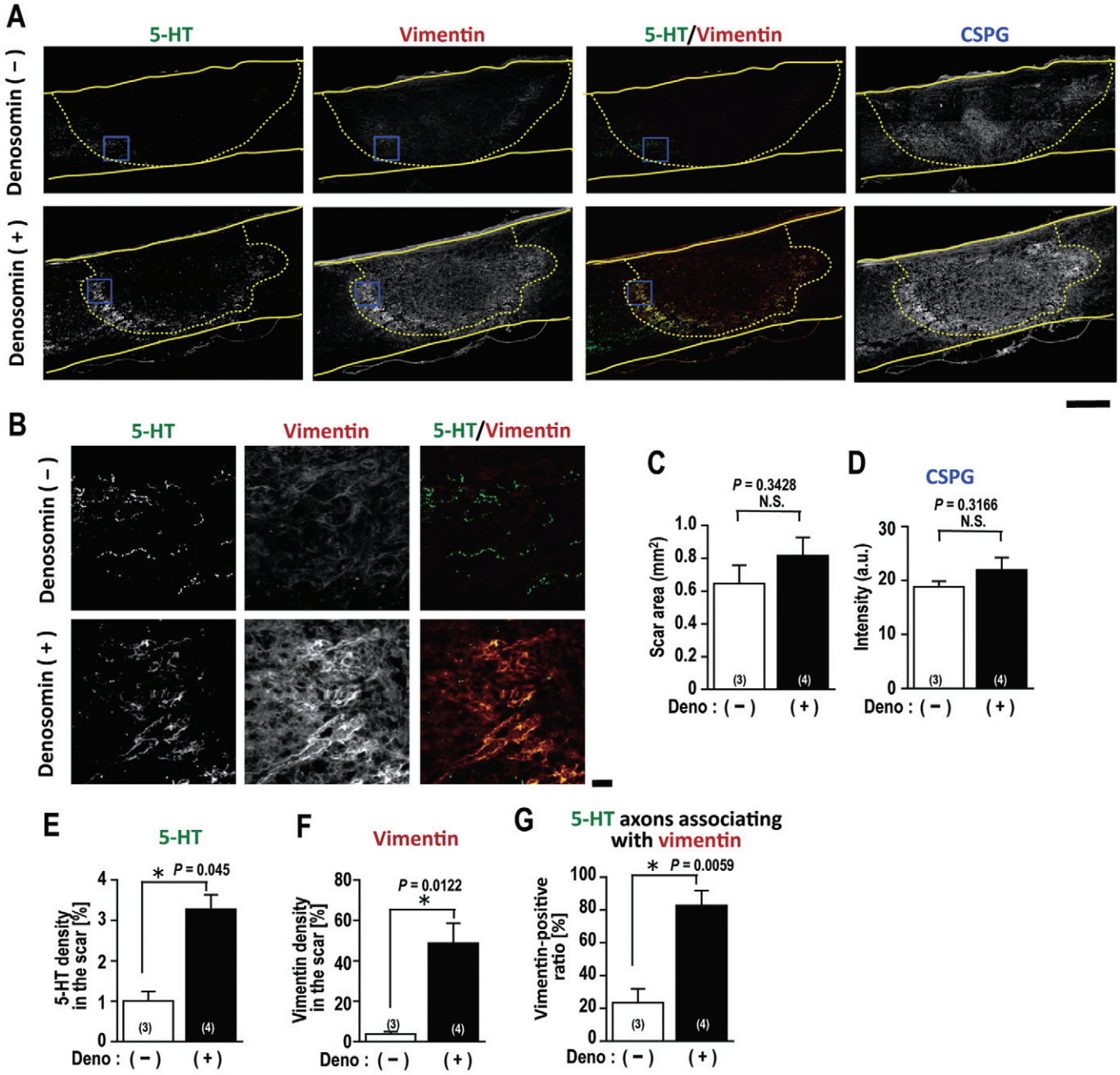

Figure 9

Denosomin-induced 5-hydroxytryptaminergic fibres associate with vimentin in SCI mice. (A,B) Spinal cord slices from SCI mice that had been treated with denosomin (Deno), or vehicle were triple immunostained for 5-HT, vimentin and CSPG. (B) Enlarged images are of insets shown in (A). The ratios of (E) 5-HT- and (F) vimentin-positive areas within the scar areas were quantified. (G) The ratio of 5-HT-positive areas associating with vimentin-positive areas were quantified. (C) The sizes of glial scars were measured. (D) The intensities for the expression of CSPG were measured. *$P < 0.05$, Student's unpaired *t*-test (two-tailed). The numbers of mice are shown in parentheses in the columns. The scale bar indicates 500 μm (A) or 20 μm (B).

Herein, we showed that denosomin can facilitate axonal elongation in primary cultured cortical neurons (Supporting Information Figure S1) and spinal cord neurons (Supporting Information Figure S2), and that denosomin also has *in vivo* activities (Figures 2, 3, 9 and 10). Specifically, denosomin facilitated the growth of axons in the injured region and improved hind limb dysfunction in SCI mice. Denosomin treatment for 7 days increased the number of 5-HT-positive axons in the lesion scar (Figure 9). Further, donosomin treatment for 14 days significantly increased 5-HT-positive axons in the caudal region, at a distance of 2 mm from the injury centre (Figure 3E and G). Although the axonal growth

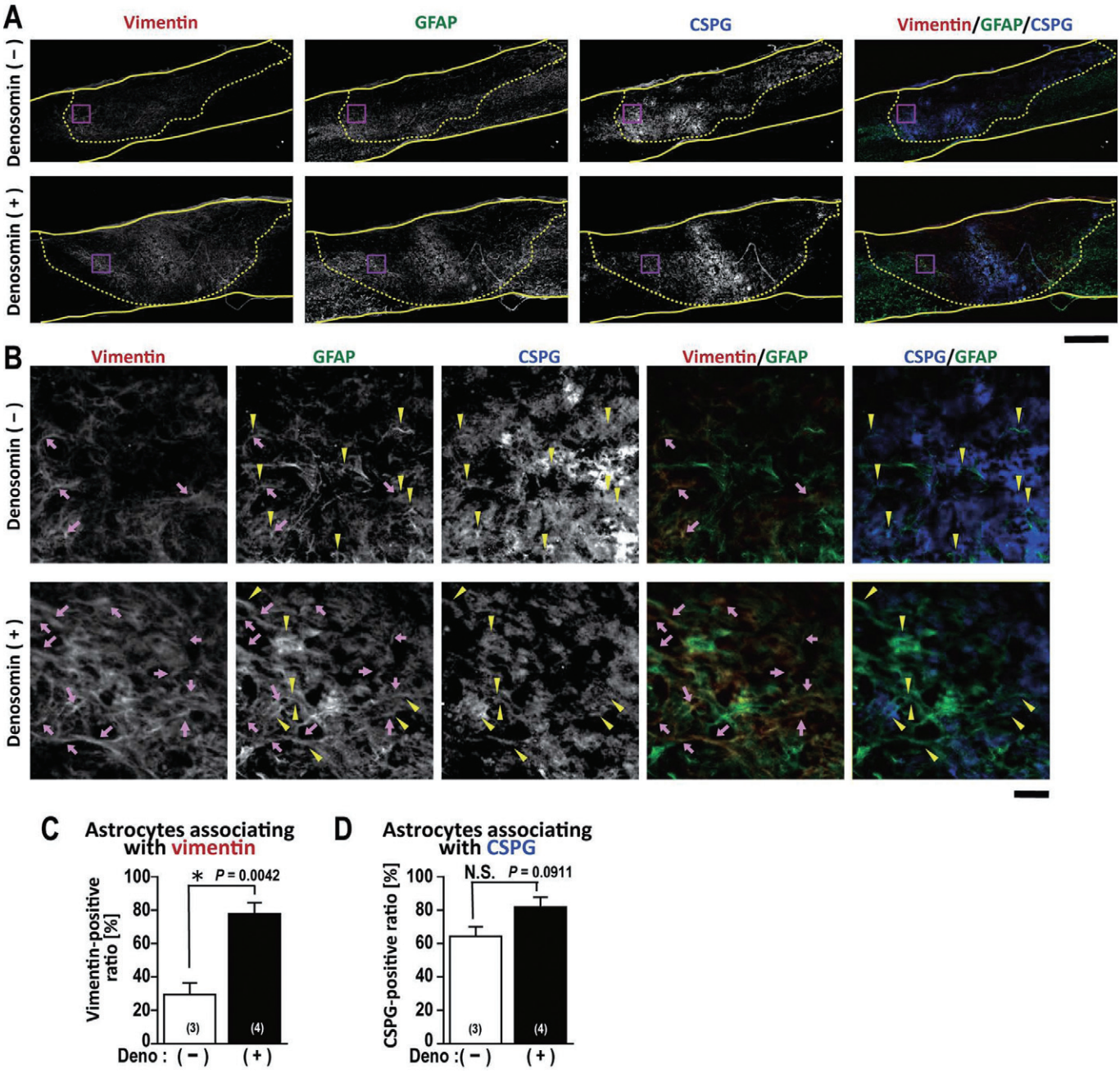

Figure 10

Denosomin-induced astrocytes associate with vimentin in SCI mice. (A,B) Spinal cord slices from SCI mice that had been treated with denosomin (Deno) or vehicle were triple immunostained for vimentin, GFAP and CSPG. (B) Enlarged images of insets shown in (A). Pink arrows indicate regions positive to vimentin and GFAP and negative to CSPG. Yellow arrowheads indicate regions positive to GFAP and CSPG and negative to vimentin. The ratios of (C) vimentin- and (D) CSPG-positive areas overlapping with the GFAP-positive astrocytes were quantified. *$P < 0.05$, Student's unpaired *t*-test (two-tailed). The numbers of mice are shown in parentheses in the columns. The scale bar indicates 500 μm (A) or 20 μm (B).

induced by denosomin in the relatively early phase may be mainly due to axonal sprouting, any extension beyond the lesion centre might be due to regeneration. Although the effects of denosomin on the BMS and BSS scores were only significant in the late phase (11–14 days after SCI), these scores also tended to be improved in denosomin-treated mice at early phase. Hence, the possibility that the neuroprotective effect of denosomin may be involved in the early phase event needs to be investigated further. We also showed that denosomin increases the expression (Figure 7G) and secretion (Figure 7H) of vimentin from astrocytes and the ratio of astrocytes that expressed vimentin (Figure 10C), which functions as an axon growth facilitator. Hence, our results indicate that administration of denosomin, p.o., induces secretion of

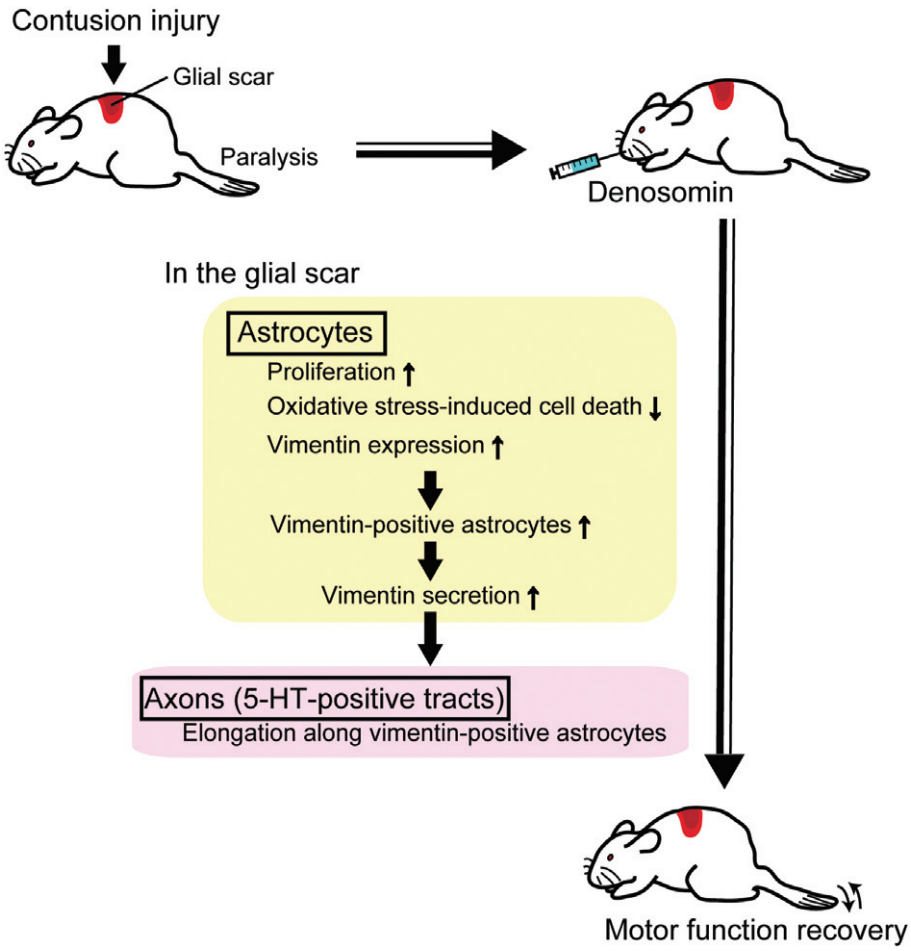

Figure 11

Schema for the effects of denosomin. Oral administration of denosomin to SCI mice induces proliferation of astrocytes, inhibits oxidative stress-induced astrocytic death and increases the vimentin expression in astrocytes. As a result, vimentin-positive astrocytes were increased, then vimentin secretion is enhanced. Secreted vimentin probably induces elongation of 5HT-positive axons, leading to hind limb motor functional recovery of SCI mice.

vimentin from astrocytes, axonal growth beyond the inhibitory glial scar and recovery of hind limb function in SCI mice (Figure 11). These also suggest a new astroglial function in the injured spinal cord, as they show that the astrocyte supports axonal growth via secretion of vimentin.

In the past, reactive astrocytes, by secreting inhibitory CSPG in the injured region of SCI, were considered to impede axonal regeneration (Silver and Miller, 2004; Yiu and He, 2006). Recently, however, it has been gradually accepted that the glial scar also has beneficial effects on CNS repair (Rolls *et al.*, 2009; White *et al.*, 2011). If the properties of astrocytes in the scar can be converted into beneficial ones, the scar would additionally support axonal growth. Vimentin as well as GFAP is the up-regulated hallmark of reactive gliosis. In animals in which vimentin has been knocked down, the size of the glial scar in SCI was found to be reduced (Xia *et al.*, 2008; Toyooka *et al.*, 2011). However, neurite length and survival of cultured cortical neurons were not influenced by vimentin knockout (Menet *et al.*, 2001) or knockdown (Desclaux *et al.*, 2009) unlike to GFAP. In addition, knockout of vimentin did not induce axon regeneration in SCI mice (Menet *et al.*, 2003). Thus, the role of vimentin in the propensity of astrocytes to induce axonal growth was not obvious. In our study, we showed that the ratio of vimentin-positive astrocytes was approximately 30% in control SCI mice and this was greatly increased by denosomin to approximately 80% (Figure 10E). Denosomin treatment also enhanced the vimentin concentration in cultured astrocytes (Figure 7F). The ratio of 5-HT axons associated with vimentin was significantly increased in the injured region of denosomin-treated SCI mice (Figure 9E). We also clarified that vimentin has an axonal elongation activity even in the presence of CSPG (Figure 7J and K). These results suggest that denosomin increases the concentration of vimentin in GFAP-positive astrocytes and this is associated with the growth of axons in the injured region of SCI mice. Other groups have reported that axonal growth is associated with vimentin-positive cells in the injured region of the spinal cord (Hsu and Xu, 2005; Busch *et al.*, 2010). Therefore, an increase in the expression of vimentin would support SCI repair.

During development, astrocytic vimentin facilitates the guidance of outgrowing corticospinal tracts (Joosten and Gribnau, 1989). Vimentin levels are known to increase after contusive injury in the spinal cord, and this increase was thought to contribute to axonal growth during spontaneous recovery (Bareyre and Schwab, 2003). Vimentin is also secreted from macrophages (Mor-Vaknin *et al.*, 2003; Xu *et al.*, 2004) as well as astrocytes (Greco *et al.*, 2010; Cordero-Llana *et al.*, 2011). Also, NG2 cells in the injured spinal cord have been reported to be positive for vimentin (Busch *et al.*, 2010). Although we have not investigated whether denosomin has an effect on macrophages and NG2 cells, our data suggest that, at least in astrocytes, denosomin induces the secretion of vimentin. However, the role and mechanism of this secreted vimentin are still not known. Although, in an ongoing study we showed that vimentin, applied to the extracellular space, elicits the phosphorylation of several signalling factors in neurons (data not shown) and propose that vimentin works like a neurotrophic factor or an adhesive factor.

We synthesized denosomin as a derivative of sominone (Matsuya *et al.*, 2009) and sominone has been found to phosphorylate RET (a receptor for glial cell line-derived neurotrophic factor, GDNF) in neurons without increasing the synthesis and secretion of GDNF (Tohda and Joyashiki, 2009). Hence, RET should be considered as a candidate for mediating the effect of denosomin in astrocytes. However, the expression of RET was not detected in astrocytes in the spinal cord (Ryu *et al.*, 2011). In addition, we found no expression of RET in astrocytes in the injured spinal cords or in naïve spinal cords (data not shown). Therefore, it is unlikely that RET is responsible for the signalling of denosomin in astrocytes. Denosomin enhances proliferation, reduces oxidative stress-induced death and promotes vimentin expression in astrocytes, leading to an increase in the number of astrocytes secreting vimentin. The secreted vimentin then probably induces axonal growth in the injured spinal cord. Other groups have reported that STAT3 (Okada *et al.*, 2006) and TGF-α (White *et al.*, 2011) signalling mediate both astrocyte proliferation and migration in SCI to enhance the healing process. However, denosomin did not affect the cellular migration of isolated astrocytes. Although the ephrin (EPHA4) receptor-mediated RhoA pathway leads to astrocyte proliferation and reactivity (Goldshmit *et al.*, 2004), EPHA4 signalling should also enhance astrocyte migration (Goldshmit and Bourne, 2010). Down-regulation experiments have indicated that vimentin is associated with astrocyte migration (Desclaux *et al.*, 2009), but the possibility that an increase in vimentin enhances astrocyte migration has not been clarified. Therefore, we think that denosomin increases vimentin without influencing astrocyte migration. We hypothesize that denosomin signalling affects astrocytes through a distinct pathway, in which STAT3, TGF-α and EPHA4 are not possibly involved . In addition to inducing astrocyte proliferation and vimentin up-regulation, denosomin is also neuroprotective (Matsuya *et al.*, 2009) and has astrocyte-protective effects (Figure 5), which suggests that denosomin has multiple beneficial effects for SCI repair. Whether all these effects of denosomin are mediated by vimentin, and the identity of its signalling pathway, are the subjects of further investigations.

The increase in reactive astrocytes associated with SCI was thought to be essentially a physical and functional barrier inhibiting axonal regeneration. However, the upregulation and secretion of vimentin converts this burden into a force for functional SCI recovery. Several pharmacotherapies for SCI are in clinical trials (Tohda and Kuboyama, 2011), but drug candidates that utilize the beneficial effects of reactive astrocytes have not been identified. Thus, denosomin, by increasing the expression and secretion of vimentin, has the potential to be used to convert the role of reactive astrocytes from one of impeding axonal growth to one of stimulating growth. This study is the first to demonstrate the beneficial role of vimentin in SCI and drug-mediated regulation of reactive astrocytes.

Acknowledgements

This work was partially supported by Grants-in-Aid for Scientific Research (C) (23500439) and Young Scientists (B) (22790246; 23700376) funding from the Japan Society for the Promotion of Science, the Expression Program, the Regional Innovation Cluster Program, a Global Type (II) grant from the Ministry of Education, Culture, Sports, Science and Technology, Japan, the Takeda Science Foundation and the Naito Foundation Natural Science Scholarship. KT, TK, MS, AN and CT designed and performed the experiments. KS synthesized denosomin. YM developed the methodology used to synthesize denosomin. KT, TK and CT prepared the manuscript. KT and TK contributed equally to this study. CT conducted the entire study. We thank Leave a Nest Co., Ltd. (Tokyo, Japan) for performing the 2D-PAGE and LC-MS/MS analyses.

Conflict of interest

The authors report no conflict interest.

References

Atta-ur-Rahman, Jamal SA, Choudhary MI (1992). Two new withanolides from *Withania somnifera*. Heterocycles 34: 689–698.

Aubert I, Ridet JL, Gage FH (1995). Regeneration in the adult mammalian CNS: guided by development. Curr Opin Neurobiol 5: 625–635.

Bareyre FM, Schwab ME (2003). Inflammation, degeneration and regeneration in the injured spinal cord: insights from DNA microarrays. Trends Neurosci 26: 555–563.

Barrett CP, Guth L, Donati EJ, Krikorian JG (1981). Astroglial reaction in the gray matter lumbar segments after midthoracic transection of the adult rat spinal cord. Exp Neurol 73: 365–377.

Basso DM, Fisher LC, Anderson AJ, Jakeman LB, McTigue DM, Popovich PG (2006). Basso Mouse Scale for locomotion detects differences in recovery after spinal cord injury in five common mouse strains. J Neurotrauma 23: 635–659.

Bignami A, Dahl D (1974). Astrocyte-specific protein and neuroglial differentiation. An immunofluorescence study with antibodies to the glial fibrillary acidic protein. J Comp Neurol 53: 27–38.

Busch SA, Horn KP, Cuascut FX, Hawthorne AL, Bai L, Miller RH *et al*. (2010). Adult NG2+ cells are permissive to neurite outgrowth and stabilize sensory axons during macrophage-induced axonal dieback after spinal cord injury. J Neurosci 30: 255–265.

Cordero-Llana O, Scott SA, Maslen SL, Anderson JM, Boyle J, Chowhdury RR *et al*. (2011). Clusterin secreted by astrocytes enhances neuronal differentiation from human neural precursor cells. Cell Death Differ 18: 907–913.

David S, Aguayo AJ (1981). Axonal elongation into peripheral nervous system 'bridges' after central nervous system injury in adult rats. Science 214: 931–933.

Davies SJ, Fitch MT, Memberg SP, Hall AK, Raisman G, Silver J (1997). Regeneration of adult axons in white matter tracts of the central nervous system. Nature 390: 680–683.

Desclaux M, Teigell M, Amar L, Vogel R, Gimenez Y Ribotta M, Privat A *et al*. (2009). A novel and efficient gene transfer strategy reduces glial reactivity and improves neuronal survival and axonal growth in vitro. PLoS ONE 4: e6227.

Eng LF (1985). Glial fibrillary acidic protein (GFAP): the major protein of glial intermediate filaments in differentiated astrocytes. J Neuroimmunol 8: 203–214.

Faulkner JR, Herrmann JE, Woo MJ, Tansey KE, Doan NB, Sofroniew MV (2004). Reactive astrocytes protect tissue and preserve function after spinal cord injury. J Neurosci 24: 2143–2155.

Goldshmit Y, Bourne J (2010). Upregulation of EphA4 on astrocytes potentially mediates astrocytic gliosis after cortical lesion in the marmoset monkey. J Neurotrauma 27: 1321–1332.

Goldshmit Y, Galea MP, Wise G, Bartlett PF, Turnley AM (2004). Axonal regeneration and lack of astrocytic gliosis in EphA4-deficient mice. J Neurosci 24: 100064–100073.

Greco TM, Seeholzer SH, Mak A, Spruce L, Ischiropoulos H (2010). Quantitative mass spectrometry-based proteomics reveals the dynamic range of primary mouse astrocyte protein secretion. J Proteome Res 9: 2764–2774.

Herrmann JE, Imura T, Song B, Qi J, Ao Y, Nguyen TK *et al*. (2008). STAT3 is a critical regulator of astrogliosis and scar formation after spinal cord injury. J Neurosci 28: 7231–7243.

Hoock TC, Newcomb PM, Herman IM (1991). β actin and its mRNA are localized at the plasma membrane and the regions of moving cytoplasm during the cellular response to injury. J Cell Biol 112: 653–664.

Hsu JY, Xu XM (2005). Early profiles of axonal growth and astroglial response after spinal cord hemisection and implantation of Schwann cell-seeded guidance channels in adult rats. J Neurosci Res 82: 472–483.

Huet D, Bagot M, Loyaux D, Capdevielle J, Conraux L, Ferrara P *et al*. (2006). SC5 mAb represents a unique tool for the detection of extracellular vimentin as a specific marker of Sezary cells. J Immunol 176: 652–659.

Jacobs BL, Martín-Cora FJ, Fornal CA (2002). Activity of medullary serotonergic neurons in freely moving animals. Brain Res Rev 40: 45–52.

Jones LL, Margolis RU, Tuszynski MH (2003). The chondroitin sulfate proteoglycans neurocan, brevican, phosphacan, and versican are differentially regulated following spinal cord injury. Exp Neurol 182: 399–411.

Joosten EA, Gribnau AA (1989). Astrocytes and guidance of outgrowing corticospinal tract axons in the rat. An immunocytochemical study using anti-vimentin and anti-glial fibrillary acidic protein. Neuroscience 31: 439–452.

Kilkenny C, Browne W, Cuthill IC, Emerson M, Altman DG (2010). NC3Rs Reporting Guidelines Working Group. Br J Pharmacol 160: 1577–1579.

Krenz NR, Weaver LC (2000). Nerve growth factor in glia and inflammatory cells of the injured rat spinal cord. J Neurochem 74: 730–739.

Kuboyama T, Tohda C, Komatsu K (2005). Neuritic regeneration and synaptic reconstruction induced by withanolide A. Br J Pharmacol 144: 961–971.

Kuboyama T, Tohda C, Komatsu K (2006). Withanoside IV and its active metabolite, sominone, attenuate Abeta(25–35)-induced neurodegeneration. Eur J Neurosci 23: 1417–1426.

McCarthy KD, de Vellis J (1980). Preparation of separate astroglial and oligodendroglial cell cultures from rat cerebral tissue. J Cell Biol 85: 890–902.

McGrath J, Drummond G, Kilkenny C, Wainwright C (2010). Guidelines for reporting experiments involving animals: the ARRIVE guidelines. Br J Pharmacol 160: 1573–1576.

McKeon RJ, Schreiber RC, Rudge JS, Silver J (1991). Reduction of neurite outgrowth in a model of glial scarring following CNS injury is correlated with the expression of inhibitory molecules on reactive astrocytes. J Neurosci 11: 3398–3411.

Matsuya Y, Yamakawa Y, Tohda C, Teshigawara K, Yamada M, Nemoto H (2009). Synthesis of sominone and its derivatives based on an RCM strategy: discovery of a novel anti-Alzheimer's disease medicine candidate 'denosomin'. Org Lett 11: 3970–3973.

Menet V, Giménez y Ribotta M, Chauvet N, Drian MJ, Lannoy J, Colucci-Guyon E *et al*. (2001). Inactivation of the glial fibrillary acidic protein gene, but not that of vimentin, improves neuronal survival and neurite growth by modifying adhesion molecule expression. J Neurosci 21: 6147–6158.

Menet V, Prieto M, Privat A, Giménez y Ribotta M (2003). Axonal plasticity and functional recovery after spinal cord injury in mice deficient in both glial fibrillary acidic protein and vimentin genes. Proc Natl Acad Sci U S A 100: 8999–9004.

Mor-Vaknin N, Punturieri A, Sitwala K, Markovitz DM (2003). Vimentin is secreted by activated macrophages. Nat Cell Biol 5: 59–63.

Okada S, Nakamura M, Katoh H, Miyao T, Shimazaki T, Ishii K *et al*. (2006). Conditional ablation of Stat3 or Socs3 discloses a dual role for reactive astrocytes after spinal cord injury. Nat Med 12: 829–834.

Olby N (2010). The pathogenesis and treatment of acute spinal cord injuries in dogs. Vet Clin North Am Small Anim Pract 40: 791–807.

Ridet JL, Malhotra SK, Privat A, Gage FH (1997). Reactive astrocytes: cellular and molecular cues to biological function. Trends Neurosci 20: 570–577.

Rolls A, Shechter R, Schwartz M (2009). The bright side of the glial scar in CNS repair. Nat Rev Neurosci 10: 235–241.

Rowland JW, Hawryluk GWJ, Kwon B, Fehlings MG (2008). Current status of acute spinal cord injury pathophysiology and emerging therapies: promise on the horizon. Neurosurg Focus 25: E2.

Ryu H, Jeon GS, Cashman NR, Kowall NW, Lee J (2011). Differential expression of c-Ret in motor neurons versus non-neuronal cells is linked to the pathogenesis of ALS. Lab Invest 91: 342–352.

Silver J, Miller JH (2004). Regeneration beyond the glial scar. Nat Rev Neurosci 5: 146–156.

Syková E, Svoboda J, Simonová Z, Jendelová P (1992). Role of astrocytes in ionic and volume homeostasis in spinal cord during development and injury. Prog Brain Res 94: 47–56.

Tohda C, Joyashiki E (2009). Sominone enhances neurite outgrowth and spatial memory mediated by the neurotrophic factor receptor, RET. Br J Pharmacol 157: 1427–1440.

Tohda C, Kuboyama T (2011). Current and future therapeutic strategies for functional repair of spinal cord injury. Pharmacol Ther 132: 57–71.

Tom VJ, Steinmetz MP, Miller JH, Doller CM, Silver J (2004). Studies on the development and behavior of the dystrophic growth cone, the hallmark of regeneration failure, in an *in vitro* model of the glial scar and after spinal cord injury. J Neurosci 24: 6531–6539.

Toyooka T, Nawashiro H, Shinomiya N, Shima K (2011). Down-regulation of glial fibrillary acidic protein and vimentin by RNA interference improves acute urinary dysfunction associated with spinal cord injury in rats. J Neurotrauma 28: 607–618.

White RE, Rao M, Gensel JC, McTigue DM, Kaspar BK, Jakeman LB (2011). Transforming growth gactor α transforms astrocytes to a growth-supportive phenotype after spinal cord injury. J Neurosci 31: 15173–15187.

Xia Y, Zhao T, Li J, Li L, Hu R, Hu S *et al.* (2008). Antisense vimentin cDNA combined with chondroitinase ABC reduces glial scar and cystic cavity formation following spinal cord injury in rats. Biochem Biophys Res Commun 377: 562–566.

Xu B, deWaal RM, Mor-Vaknin N, Hibbard C, Markovitz DM, Kahn ML (2004). The endothelial cell-specific antibody PAL-E identifies a secreted form of vimentin in the blood vasculature. Mol Cell Biol 24: 9198–9206.

Yiu G, He Z (2006). Glial inhibition of CNS axon regeneration. Nat Rev Neurosci 7: 617–627.

Supporting information

Additional Supporting Information may be found in the online version of this article:

Figure S1 Denosomin enhances axonal outgrowth in primary cerebrocortical cultures. Rat primary cultured cerebrocortical cells were cultured in the presence or absence of 1 μM denosomin (Deno) for 6 days. Subsequently, the cortical neurons were immunostained for pNF-H and MAP2 and counterstained with DAPI (A). The densities of pNF-H-positive axons per neuron were quantified (B). The distribution of neurons and non-neuronal cells per 0.1 mm^2 was evaluated by the quantification of MAP2- and DAPI-positive cells (C). MAP2- and DAPI-positive cells were defined as neurons. MAP2-negative and DAPI-positive cells were defined as non-neuronal cells. *$P < 0.05$, Student's unpaired *t*-test (two-tailed). N.S., not significant. The numbers of photos are bracketed in columns. The scale bar indicates 100 μm.

Figure S2 Denosomin enhances axonal outgrowth and the proliferation of non-neuronal cells in primary spinal cord cultures. (A, B) Rat primary cultured spinal cord cells were cultured in the presence or absence of 1 μM denosomin (Deno) for 4 days. Subsequently, the spinal cord neurons were immunostained for pNF-H (A) and MAP2. The densities of the pNF-H-positive axons per neuron were quantified (B). (C–F) Five days after treatment with or without 1 μM denosomin (Deno), BrdU was applied to the spinal cord cells for 24 h. Subsequently, the cells were immunostained for MAP2 and BrdU and counterstained with DAPI (C). Cellular distributions of neurons and non-neuronal cells per 0.1 mm^2 were evaluated by the quantification of MAP2- and DAPI-positive cells (D). The proliferation of non-neuronal cells was evaluated by the quantification of BrdU-positive and MAP2-negative cells (E). The growth rate of non-neuronal cells was evaluated by the ratio of BrdU-positive cells to MAP2-negative cells (F). Arrows indicate the proliferating non-neuronal cells. *$P < 0.05$, Student's unpaired *t*-test (two-tailed). The numbers of photos are shown in parentheses in the columns. The scale bar indicates 100 μm.

Figure S3 2D-PAGE analysis reveals a dense spot increased by denosomin treatment in cultured astrocytes. (A, B) Cultured rat astrocytes were treated with vehicle solution or 1 μM denosomin for 6 days. After the cells were lysed, the lysates were degenerated and analysed with 2D-PAGE. (B) Enlarged images were in insets in (A). The spots enclosed in dashed line in (B) were digested with trypsin and analysed with LC/MS/MS. The spots were identified as rat vimentin (NP_112402) by the Mascot Search (protein sequence coverage: 43%; Matrix Science).

Movie S1 Movie of vehicle-administered SCI mice on the 14th postoperative day.

Movie S2 Movie of denosomin-administered SCI mice on the 14th postoperative day.